NASA
Technical
Memorandum

NASA TM - 103580

TESTING AND ANALYSES OF ELECTROCHEMICAL CELLS USING FREQUENCY RESPONSE

Center Director's Discretionary Fund Final Report, Project No. 90-18

By D.L. Thomas and O.A. Norton Jr.

Information and Electronic Systems Laboratory
Science and Engineering Directorate

March 1992

NASA

National Aeronautics and
Space Administration

George C. Marshall Space Flight Center

REPORT DOCUMENTATION PAGE

1. AGENCY USE ONLY (Leave blank)	2. REPORT DATE	3. REPORT TYPE AND DATES COVERED
	March 1992	Technical Memorandum

4. TITLE AND SUBTITLE

Testing and Analyses of Electrochemical Cells Using Frequency Response—Center Director's Discretionary Fund Final Report, Project No. 90-18

5. FUNDING NUMBERS

6. AUTHOR(S)

O.A. Norton, Jr. and D.L. Thomas*

7. PERFORMING ORGANIZATION NAME(S) AND ADDRESS(ES)

George C. Marshall Space Flight Center
Marshall Space Flight Center, Alabama 35812

8. PERFORMING ORGANIZATION REPORT NUMBER

9. SPONSORING / MONITORING AGENCY NAME(S) AND ADDRESS(ES)

National Aeronautics and Space Administration
Washington, DC 20546

10. SPONSORING / MONITORING AGENCY REPORT NUMBER

NASA TM-103580

11. SUPPLEMENTARY NOTES

Prepared by Information and Electronic Systems Laboratory, Science and Engineering Directorate.
*University of Alabama, Huntsville

12a. DISTRIBUTION / AVAILABILITY STATEMENT

Unclassified — Unlimited

12b. DISTRIBUTION CODE

13. ABSTRACT (Maximum 200 words)

The feasibility of electrochemical impedance spectroscopy as a method for analyzing battery state of health and state of charge was investigated. Porous silver, zinc, nickel, and cadmium electrodes as well as silver/zinc cells were studied. State of charge could be correlated with impedance data for all but the nickel electrodes. State of health was correlated with impedance data for two silver/zinc cells, one apparently good and the other dead. The experimental data were fit to equivalent circuit models.

14. SUBJECT TERMS

Impedance spectroscopy on silver, cadmium, nickel, and zinc electrodes.

15. NUMBER OF PAGES

23

16. PRICE CODE

NTIS

17. SECURITY CLASSIFICATION OF REPORT	18. SECURITY CLASSIFICATION OF THIS PAGE	19. SECURITY CLASSIFICATION OF ABSTRACT	20. LIMITATION OF ABSTRACT
Unclassified	Unclassified	Unclassified	Unlimited

TABLE OF CONTENTS

LIST OF ILLUSTRATIONS

iv

LIST OF ILLUSTRATIONS (Continued)

TECHNICAL MEMORANDUM

TESTING AND ANALYSES OF ELECTROCHEMICAL CELLS USING FREQUENCY RESPONSE

Center Director's Discretionary Fund Final Report, Project No. 90-18

INTRODUCTION

This report presents the research performed for NASA-MSFC during the period from February 1 to December 31, 1991, under contract No. NAS8-36955-114. The objective of this project was to investigate the feasibility of using frequency response techniques for enhancing destructive physical analysis and for nondestructive testing of aerospace battery electrodes. Nickel, cadmium, silver, and zinc electrodes were tested by imposing alternating current upon the electrodes and measuring the magnitude and phase of the response voltage. This yields an impedance spectrum for the battery electrode from which electrochemical kinetic, double-layer capacitance, and mass transfer effects can be characterized. Frequencies from 10 kHz to 0.1 mHz were used in the testing.

EXPERIMENTAL

Figure 1 shows a diagram of the experimental apparatus. The centerpiece is a Schlumberger model 1250 frequency response analyzer (FRA) and model 1286 electrochemical interface (EI). The FRA contains a signal generator, the output of which can modulate the voltage or current output of the EI. The FRA also has two signal inputs which are connected to the two analog outputs of the EI, proportional to the cell current and the electrode potential.
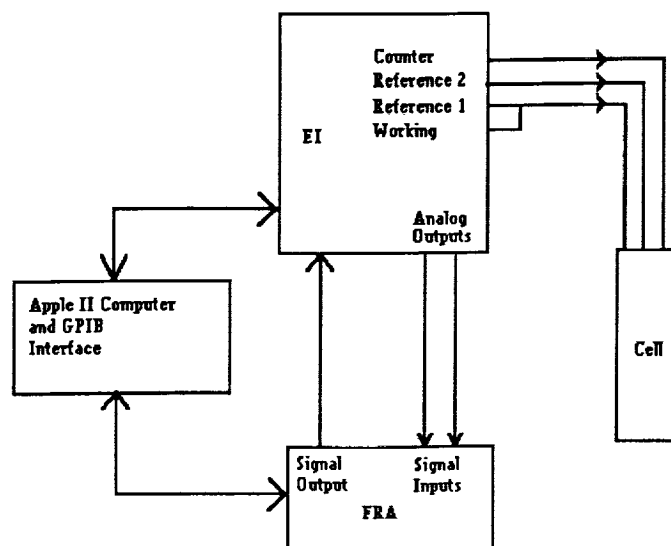

Figure 1. Diagram of the experimental apparatus.

The battery electrodes were placed in prismatic cells fabricated from Plexiglas. These cells typically contained one working electrode and one or two counterelectrodes. The working electrode potential was measured relative to a reference electrode that was also in the cell. Only a small amount of current, on the order of microamperes, is drawn from the reference electrode during potential measurements, hence the working electrode polarization can be measured without interference from the counterelectrode. A silver reference electrode was used for silver and zinc working electrode measurements, while a nickel reference electrode was used for nickel and cadmium electrode measurements.

The FRA and EI were controlled by an Apple II computer through a GPIB interface. Programs written in Applesoft Basic were used to control the amplitude and frequency during logarithmic sweeps of the working electrode impedance versus frequency, and to control the EI during charge and discharge of the cells. The results were displayed on the computer screen and recorded in a notebook for processing. Bode magnitude plots (impedance magnitude versus log frequency) and Bode angle plots (impedance phase angle versus log frequency) were used to represent the data.

Frequency response analysis is valid only for linear systems, but electrochemical parameters such as interfacial resistance, double-layer capacitance, and diffusion (Warburg) impedance are strong functions of potential. Hence, it is important that the amplitude of the voltage response be small. Each of the above named impedances can be treated as constant if the voltage amplitude driving current through that impedance does not exceed 5 mV. The computer programs were written so that the total working electrode voltage amplitude was about 5 mV, thus the amplitude through the individual impedances would be no larger than this maximum permissible value.

MATHEMATICAL MODELING

This section briefly summarizes the modeling techniques for analyzing impedance data. More complete presentations can be found in the literature.[1] Two techniques are reported—equivalent circuit analysis and finite difference numerical analysis. Most of the work in this project used the first technique, but work with the second technique was begun.

Equivalent Circuit Analysis

The traditional approach to electrochemical impedance data is to model it in terms of equivalent electrical circuit elements, fitting the experimental data to the circuit with the method of least squares. Equivalent circuit elements used in this work will be discussed briefly.

The double-layer capacitance (C_d) of the electrode/solution interface is usually modeled as a pure capacitance. The double layer itself is a solution layer, about 10 to 20 Å thick, adjacent to the electrode surface which can be charged due to (1) nonrandom alignment of dipoles near or at the electrode surface or (2) preferential adsorption of either the anion or cation at the electrode surface. This capacitance is relatively large, on the order of 10^{-5} F/cm^2, and is strongly potential dependent, but can be treated as constant for potential variations of the order of 5 mV or less.[2]

There are two electrochemical phenomena that can be modeled as pure resistance with no reactive component: ohmic electrolyte resistance and Faradaic resistance. the ohmic electrolyte resistance R_Ω is usually linear over the entire range of potential and is simple to analyze. In the case

of alkaline aerospace batteries, the electrolyte conductivity is quite high so that R_Ω is low. The Faradaic resistance R_F is the resistance to charge transfer across the electrode/electrolyte interface and is also known as the kinetic resistance. It is highly nonlinear since the relationship between electrode reaction rate (current density) and interfacial potential difference is exponential, but the exponential relationship can be linearized for potential variations of about 5 mV or less.

The Warburg impedance is caused by concentration gradients in the mass transfer boundary layer (thickness of 100 μm order of magnitude) adjacent to an electrode, has both resistive and reactive components, and increases as frequency decreases. This impedance becomes appreciable when the frequency is low enough that significant depletion of reactants or accumulation of products occurs during the anodic or cathodic half of a sinusoid. The Warburg impedance for an electrode in a large excess (semi-infinite) of solution is

$$Z_w = \sigma/(j\omega D)^{0.5} , \qquad (1)$$

where D is the diffusion coefficient, ω is the frequency, and σ is the Warburg coefficient,

$$\sigma = RT/C_b(nF)^2 , \qquad (2)$$

R is the gas constant, T the absolute temperature, C_b the bulk concentration, n the stoiciometric number of electrons transferred, and F is Faraday's constant (96,487 Coulombs/mole electrons). The phase of the Warburg impedance is $-45°$, and the magnitude is proportional to the inverse square root of frequency. More complex expressions are required when there is not excess solution or when there is more than one diffusing species contributing to the impedance. An exponential relation between concentration and potential (the Nernst equation or something similar) means that this impedance is also highly nonlinear but can be linearized for voltage amplitudes less than 5 mV.

Another circuit element has gained popularity in recent years, especially when the data to be analyzed does not fit simple circuit elements, is the constant phase element (CPE). It has the mathematical form

$$Z_{cpe} = A(jw)^m , \qquad (3)$$

where A and n are constants that can be fit to experimental data. The impedances R_Ω, R_F, C_d, and Z_w can be thought of as CPE's where m is a theoretical value. The CPE can be used to account for complex phenomena such as coupled diffusion effects or porosity fluctuations. It is often used as an empirical fitting device and has the disadvantages associated with such tools. However, if the alternative is an equivalent circuit with an excessive number of elements (circuits with 15 or 20 elements have been proposed in some systems without physical explanations of the elements) then the CPE may be an attractive alternative.

Figure 2a shows a simple equivalent circuit that has been used often. C_d is considered parallel to R_f and Z_w, forming an equivalent interfacial impedance that is in series with the R_Ω. The justification cited is that the first three can only be determined by measurements at an interface. However, since R_f and C_d are double-layer phenomena while Z_w is a diffusion layer phenomena (orders of magnitude thicker than the double-layer), the circuit of figure 2b seems more physically realistic.
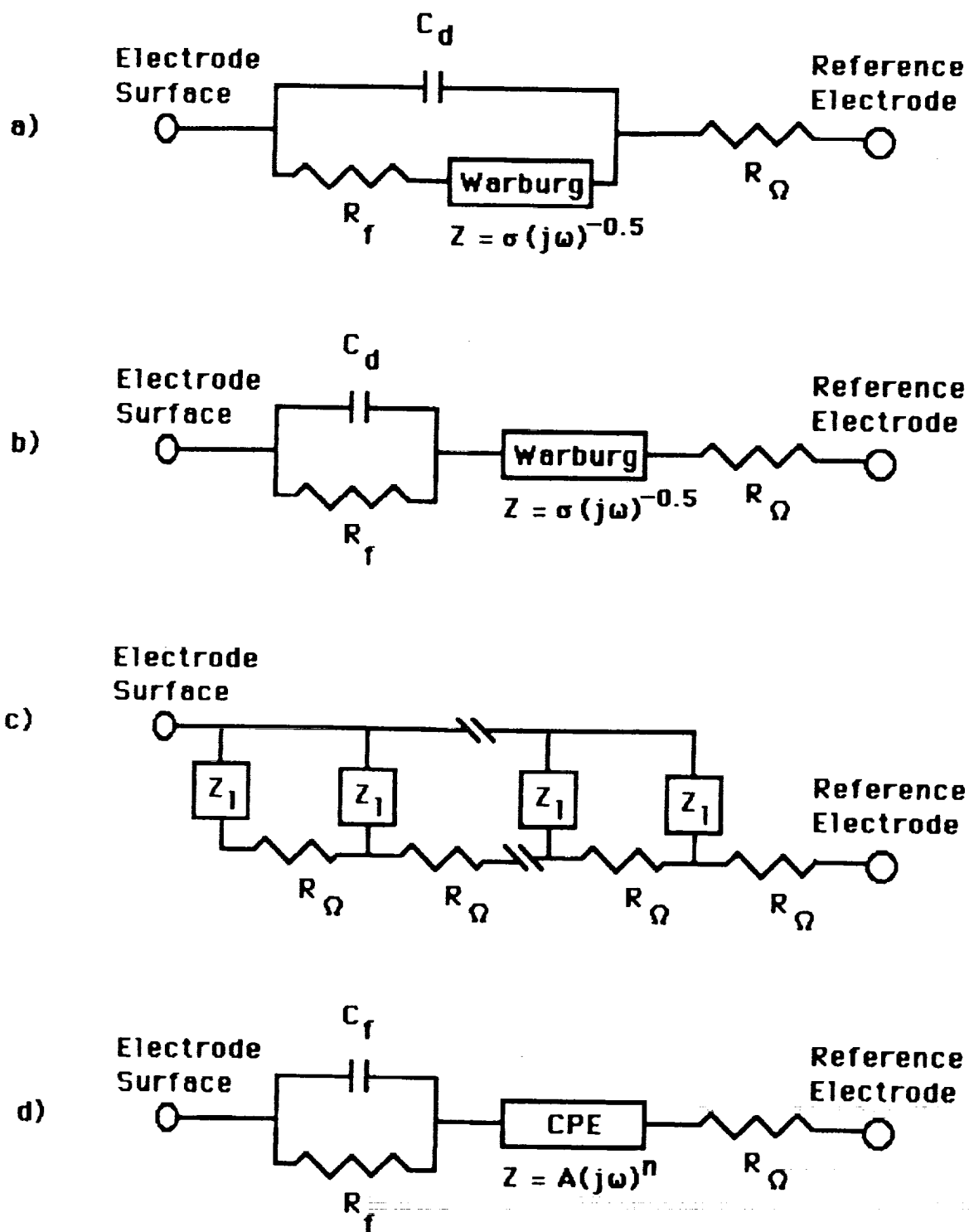
Figure 2. Equivalent circuits used in impedance modeling.

4

The two preceding equivalent circuits are for smooth planar electrodes. Battery electrodes usually are porous electrodes in which there is pore electrolyte resistance as well as the interfacial impedances discussed in the preceding paragraphs. Figure 2c shows the transmission line model that is often used to model porous electrodes, where R_Ω is the pore electrolyte resistance and Z_1 represents the collective interfacial impedances. The impedance of this electrode, where there is no direct current bias current and no concentration gradients along the pore axis,[3] is

$$Z_p = \cosh{(mL)}/(\kappa_{eff}m \sinh{(mL)}) \ , \tag{4}$$

where

$$m^2 = a/\kappa_{eff}Z_i \ , \tag{5}$$

a is the interfacial surface area per unit volume and κ_{eff} is the effective conductivity of the electrolyte. In the limit of small mL

$$Z_p = Z_1/aL \ , \tag{6}$$

while in the limit of large mL

$$Z_p = 1/\kappa_{eff}m \ . \tag{7}$$

At this latter limit, the phase angle of Z_1 is halved so that the double-layer capacitance has an apparent phase angle of $-45°$ while semi-infinite Warburg impedance has an angle of $-22.5°$

The equivalent circuit for Z_1 used most in this study is shown in figure 2d, and is similar to figure 2b except that the Warburg impedance was replaced by a CPE and the ohmic resistance was deleted. Also, almost all the phase angles measured were less than zero (capacitive reactance), and, when it is said that a phase angle increases, it is referring to the magnitude of the angle.

Numerical Finite Difference Models

The physics and chemistry that govern battery electrode operation can be expressed in the form of coupled differential equations with much greater clarity and flexibility than is possible using equivalent circuit techniques. In particular, complicated phenomena that would otherwise get lumped into CPE's can be modeled in this way. Numerical finite difference solutions for models of charging or discharging batteries abound in the literature. However, these techniques have not been widely utilized to analyze impedance data.

RESULTS AND DISCUSSION

Silver/Zinc Cells

A cell consisting of one silver and one zinc electrode from a Yardney 50-Ah battery was assembled and tested. The reference electrode was an anodized silver wire that was connected to the silver working electrode during cycling. The cell was cycled twice, with discharge at 100 percent

5

of measured capacity, and the impedance spectrum of each electrode was measured at 100, 75, 50, 25, and 0 percent states of charge (SOC).

Figures 3 and 4, respectively, are the Bode magnitude and angle plots for the silver electrode during discharge on the second cycle. It shows a trend of decreasing magnitude and phase angle with increasing state of charge at low frequency, reflecting increased mass transfer impedance, although most of the lines cross at 3 mHz. These general trends were observed in both cycles. Figures 5 and 6 are the plots for the zinc electrode during discharge on the second cycle. In this case, the fully charged state has the highest impedance magnitude and phase angle. In both electrodes it seems that the bare metal in contact with solution has the higher impedance, while the metal with the fully oxidized surface has the lowest impedance.

Tests were also made with two Yardney 150-Ah cells. These cells had been cycled at least 100 times, and, as received, had rest potentials of 1.6 V (cell No. 1) and 0.3 V (cell No. 2). Impedance measurements were first made for the two cells as received and shown in figures 7 and 8. Cell No. 2 had a much higher low-frequency impedance. It is thought that the zinc electrode morphology in this cell had deteriorated, reducing the zinc active surface area and increasing the mass transfer limitations. The cells were then charged to 1.8 V rest potential, and spectra were again run and are shown in figures 9 and 10. Charging increased the magnitude of the impedance for both cells but caused the phase angles to become less negative at low frequency. The work reported in the previous paragraph showed that impedance magnitude is highest for bare metal electrodes (the zinc electrode in this case), hence the zinc electrode impedance increases more than the silver electrode impedance decreases during charge. It is also interesting to note that the charged cell has positive phase angles at high frequency. It has been shown in other systems[1][4][5] that this can result from nonelementary electrochemical reactions. This most likely occurs at the zinc electrode in which the reaction product, zincate ion, is quite soluble in the electrolyte solution.

Figures 11 and 12 compare the experimental results for the impedance of a discharged silver electrode with the best fit to the equivalent shown in figure 2d at the limit given by equation (6). The circuit seems capable of following the trends in the magnitude, while the maximum angle discrepancy is about 0.25°. Table 1 gives values for the equivalent circuit parameters. The parameter aC, which is the capacitance per unit volume, is a figure of merit that characterizes the electrochemically active surface area.

Nickel/Cadmium Cells

Impedance spectroscopy was used by Armstrong et al.[6] and Armstrong and Edmondson[7] to study cadmium electrodes while Lenhart et al.[8] have studied porous nickel electrodes. Ni-Cd cell studies have been performed by Sathyanarayana et al.[9] and Zimmerman et al.[10]

A cell consisting of a nickel electrode sandwiched between cadmium electrodes was constructed, and impedance spectra for the nickel and cadmium electrodes were obtained. Figures 13 and 14 compare the spectra for charged and discharged cadmium electrodes. As with the zinc and silver electrodes, the low-frequency impedance magnitude and phase angles for the bare metal (charged cadmium) are higher than for the oxidized metal. There was little observed dependance of impedance with SOC for the nickel electrode, which is always in an oxidized state.

Figures 15 and 16 compare the cadmium electrode experimental impedance (fig. 2d) with the equivalent circuit best fit. Of all the electrodes studied, this one seemed to fit the equivalent circuit

6

best. Figures 17 and 18 compare the results for the nickel electrodes, which give a fairly reasonable agreement between experiment and equivalent circuit. There is some discrepancy in the angle plot although the trends are comparable. The results are markedly different from Lenhart et al.,[8] who reported all positive phase angles for porous nickel electrodes over approximately the same frequency range. This may be due to the presence of Li-Oh in the electrolyte and to differences in electrode manufacture.

It should be emphasized that the fit of equivalent circuits to experiments were obtained by replacing the Warburg impedance, which is based on fundamental electrochemical transport principles, with the empirical constant phase element. Replacement of equivalent circuit models with coupled differential equation models is recommended for future studies. While this approach is much more difficult to implement, it is expected to provide a more rigorous understanding of porous battery electrodes.

It is also interesting to note the wide variation in aC values in table 1. It is possible that the CPE is also accounting for some or most of the double-layer capacitance effects, and that a more fundamental modeling approach will yield double-layer capacitances that do not differ by so many orders of magnitude. However, other workers have also observed order of magnitude differences in capacitance effects between electrodes. For instance, Tiedemann and Newman,[11] using models without empirical components, observed that capacitance effects for porous lead electrodes are two orders of magnitude higher than for porous lead dioxide electrodes. This is because double layer capacitance is a chemical and not purely an electrical effect.

CONCLUSIONS

1. State of charge estimations can be made using electrochemical impedance techniques. In particular, the low-frequency impedance of metal electrodes is higher in the fully reduced state than in the fully oxidized state.

2. Comparisons between healthy and unhealthy Ag-Zn cells show that, at least in some instances, state of health can be correlated with impedance data. The "dead cell," which presumably failed because of decreased active zinc content and decreased active zinc surface area, had a significantly higher low frequency impedance.

3. Semi-empirical equivalent circuit models were able to fit the experimental data. It is recommended that models incorporating the fundamental coupled-differential equations describing the electrodes be solved in future work. Such an approach will be more difficult, and will require significant time and resources to initiate, but the results will be more fundamentally satisfying.
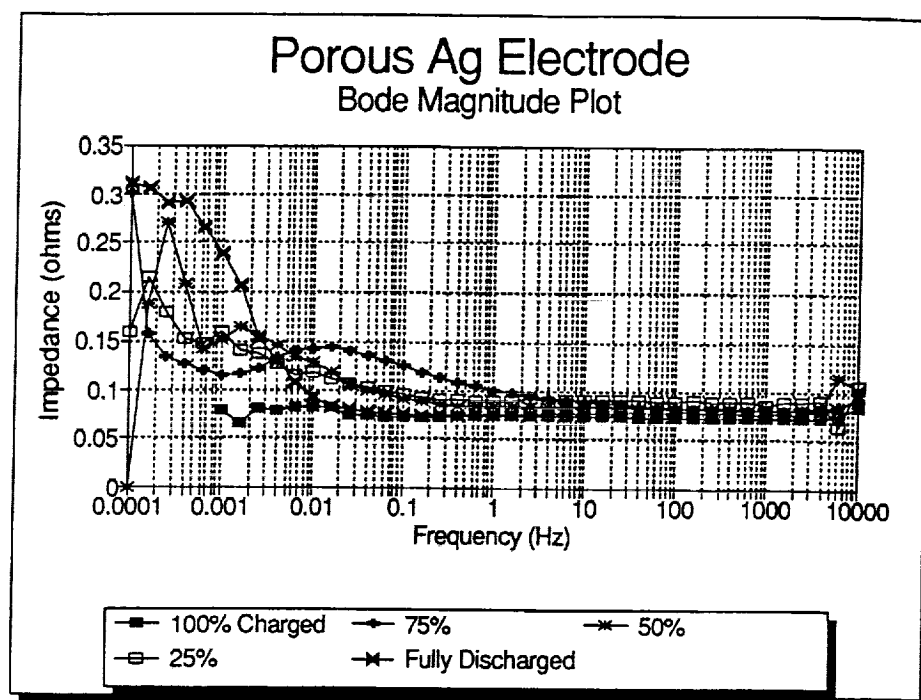
7

Figure 3. Bode magnitude plot of porous silver electrode (169 cm^2) impedance as a function of state of charge.
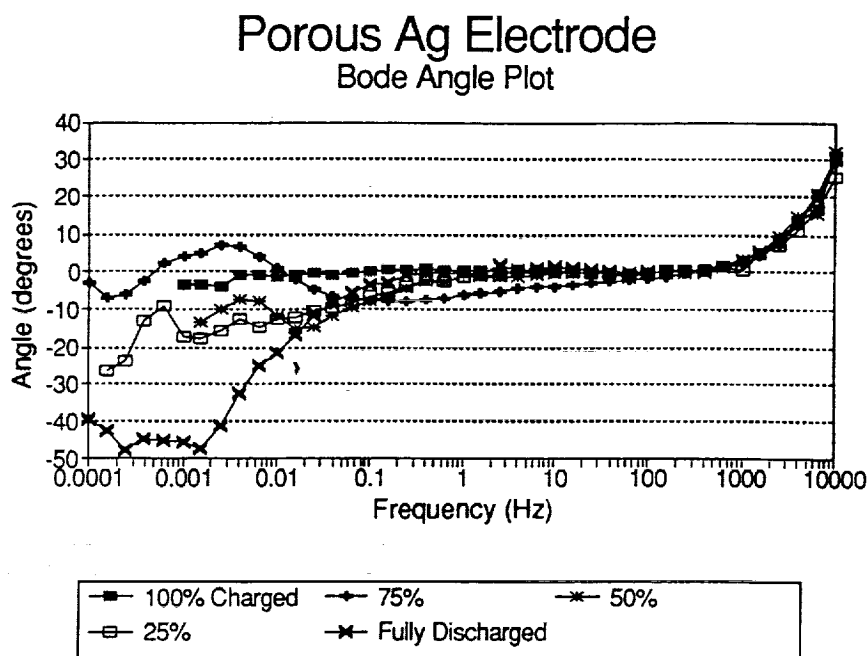

Figure 4. Bode angle plot of porous silver electrode (169 cm^2) impedance as a function of state of charge.
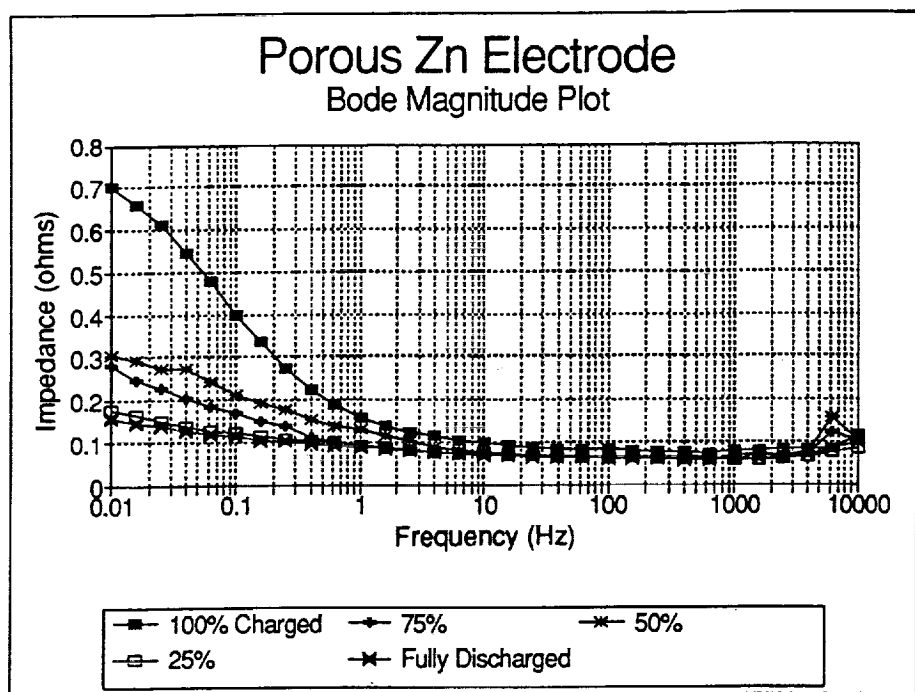
Figure 5. Bode magnitude plot of porous zinc electrode (169 cm^2) impedance as a function of state of charge.
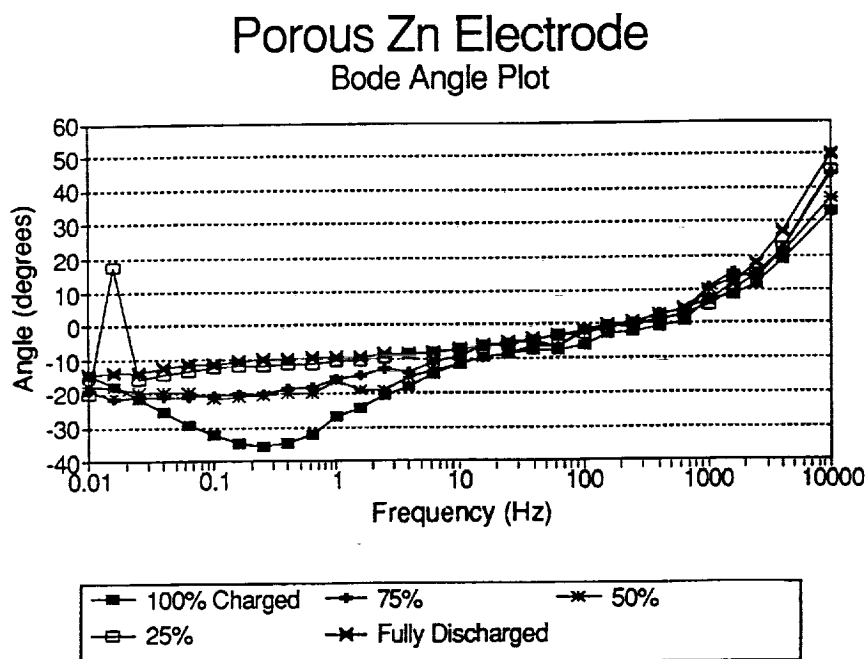

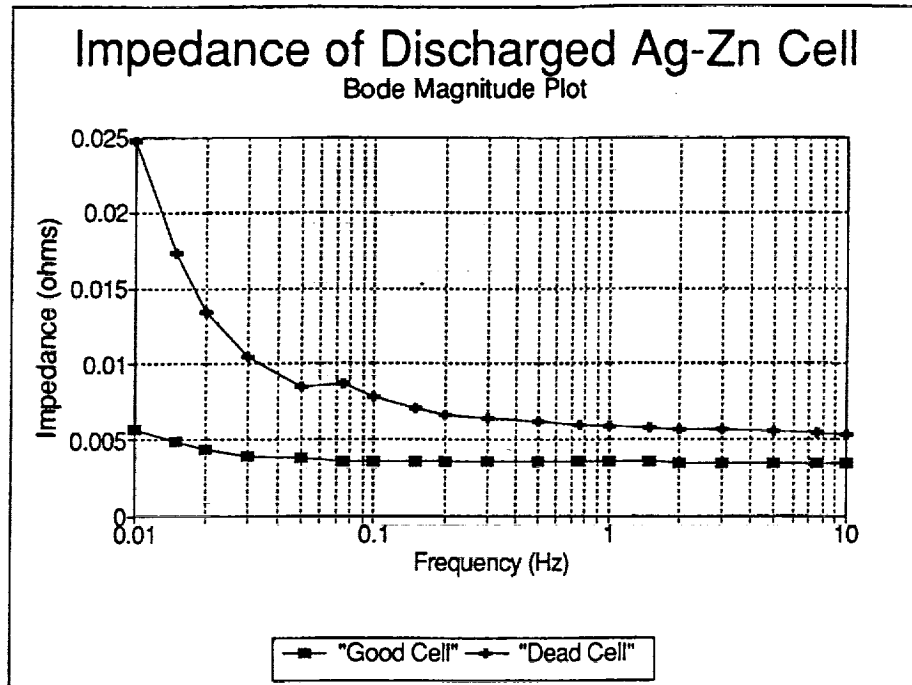Figure 6. Bode angle plot of porous zinc electrode impedance (169 cm^2) as a function of state of charge.

Figure 7. Comparison of discharged silver/zinc cell impedance for a good cell
and a dead cell (Bode magnitude plot).

Figure 8. Comparison of discharged silver/zinc cell impedance for a good cell
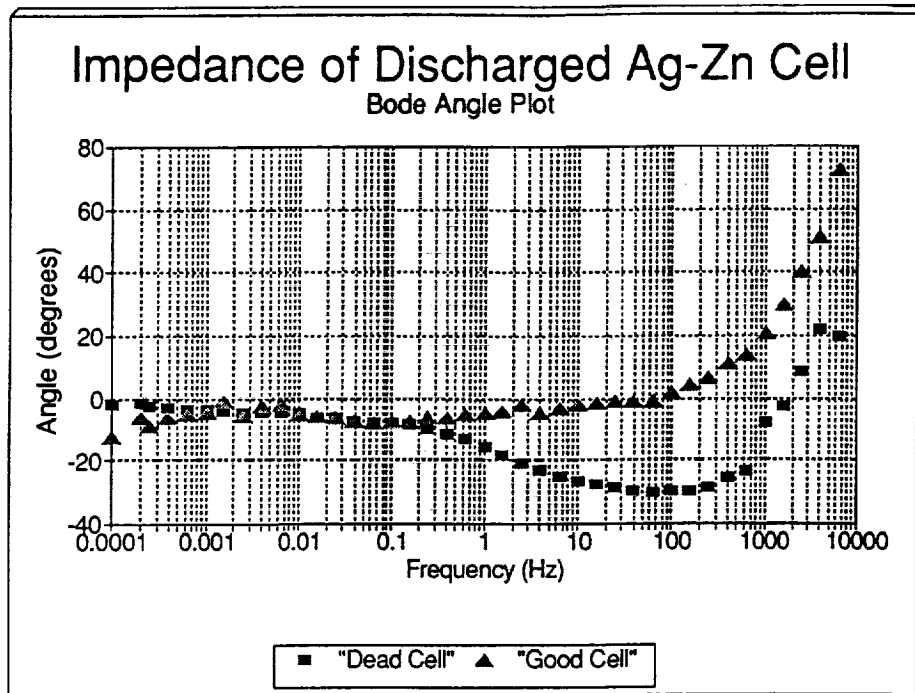and a dead cell (Bode angle plot).

10

Figure 9. Comparison of charged silver/zinc cell impedance for a good cell
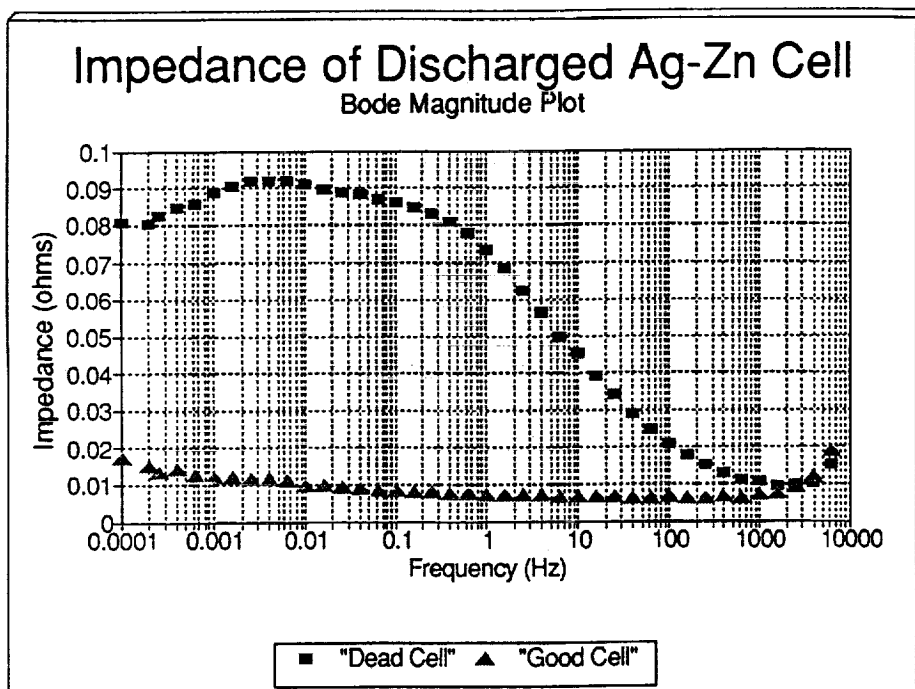and a dead cell (Bode angle plot).

Figure 10. Comparison of charged silver/zinc cell impedance for a good cell
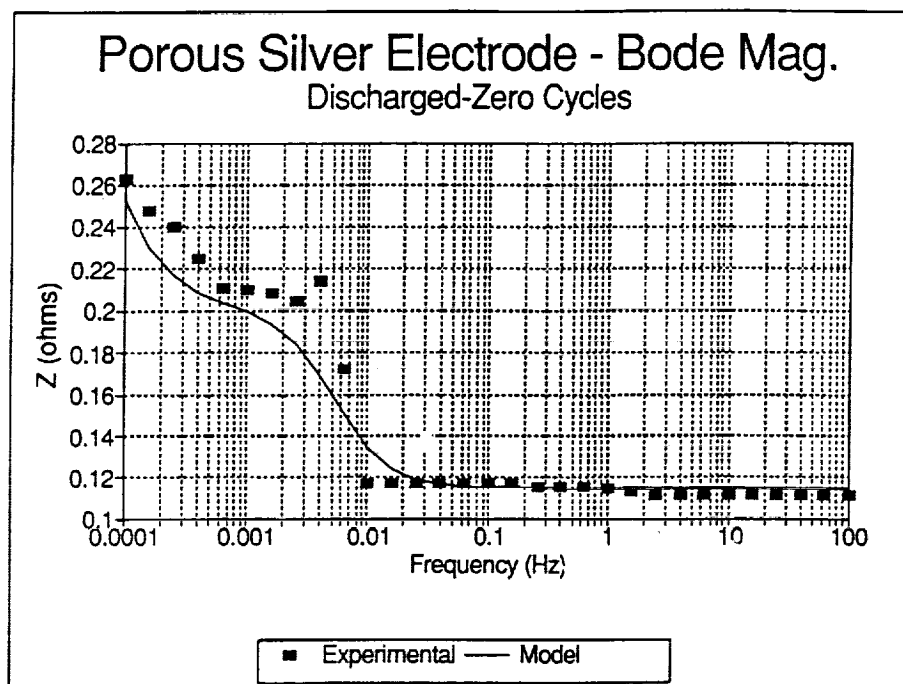and a dead cell (Bode magnitude plot).

Figure 11. Comparison of experimental and equivalent circuit impedance
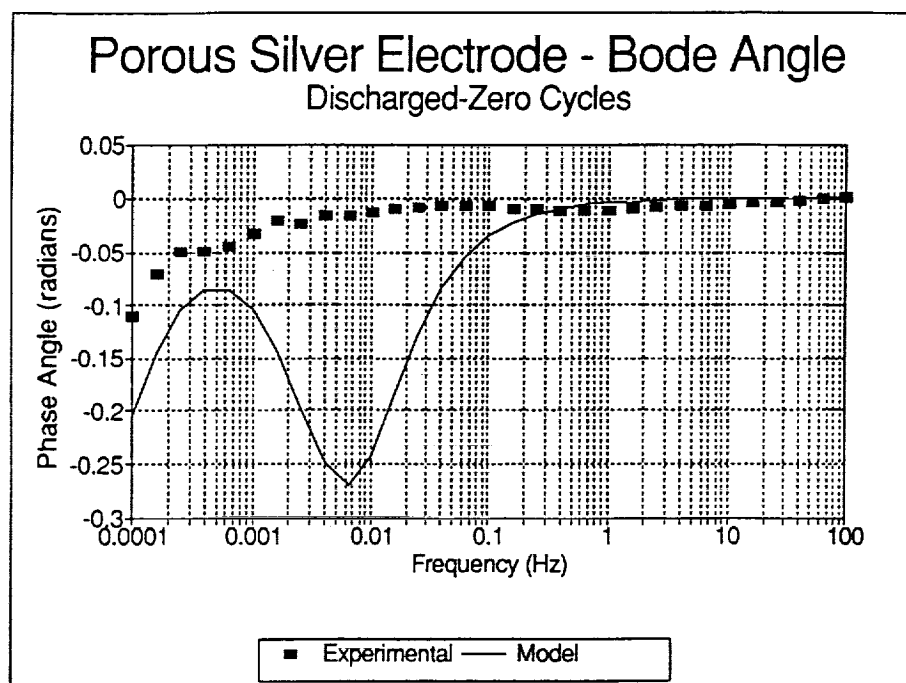for a (169 cm²) charged silver electrode (Bode magnitude plot).

Figure 12. Comparison of experimental and equivalent circuit impedance
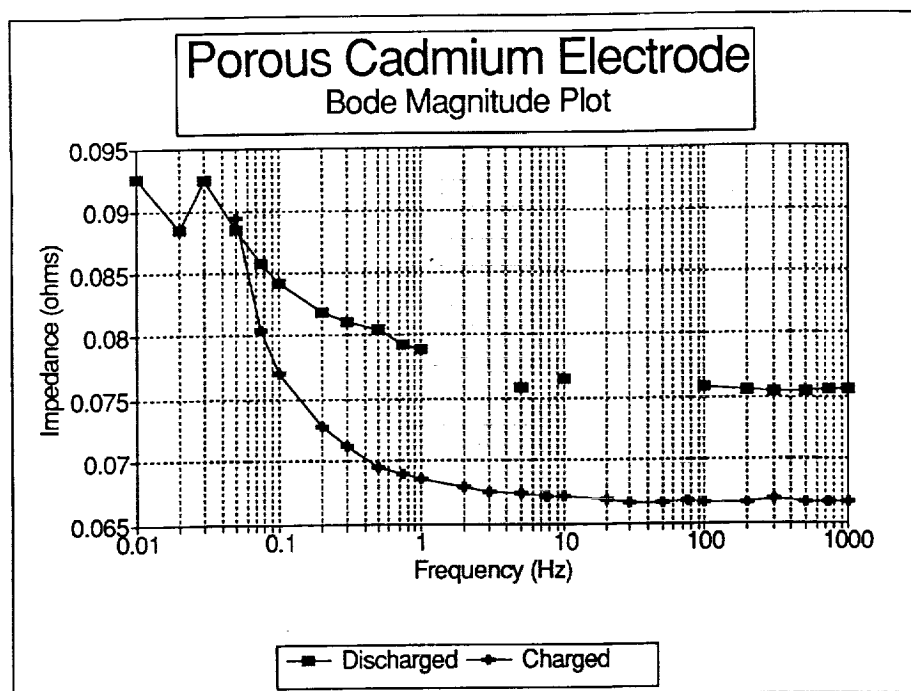for a (169 cm²) discharged silver electrode (Bode angle plot).

Figure 13. Bode magnitude plot of porous cadmium electrode (230 cm²) impedance as a function of state of charge.
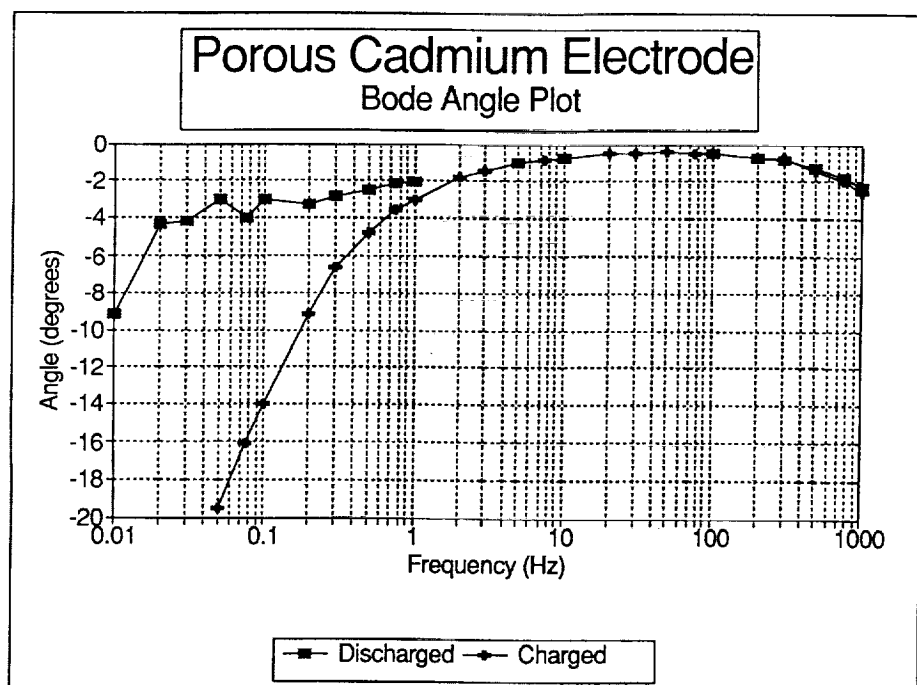

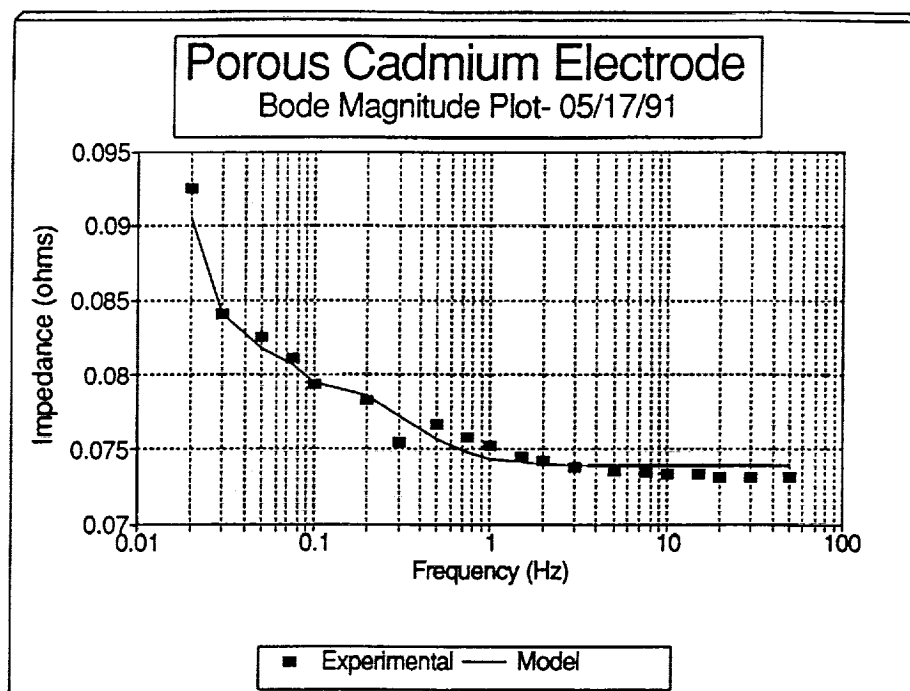Figure 14. Bode angle plot of porous cadmium electrode (230 cm²) impedance as a function of state of charge.

Figure 15. Comparison of experimental and equivalent circuit impedance for a charged cadmium (230 cm^2) electrode (Bode magnitude plot).
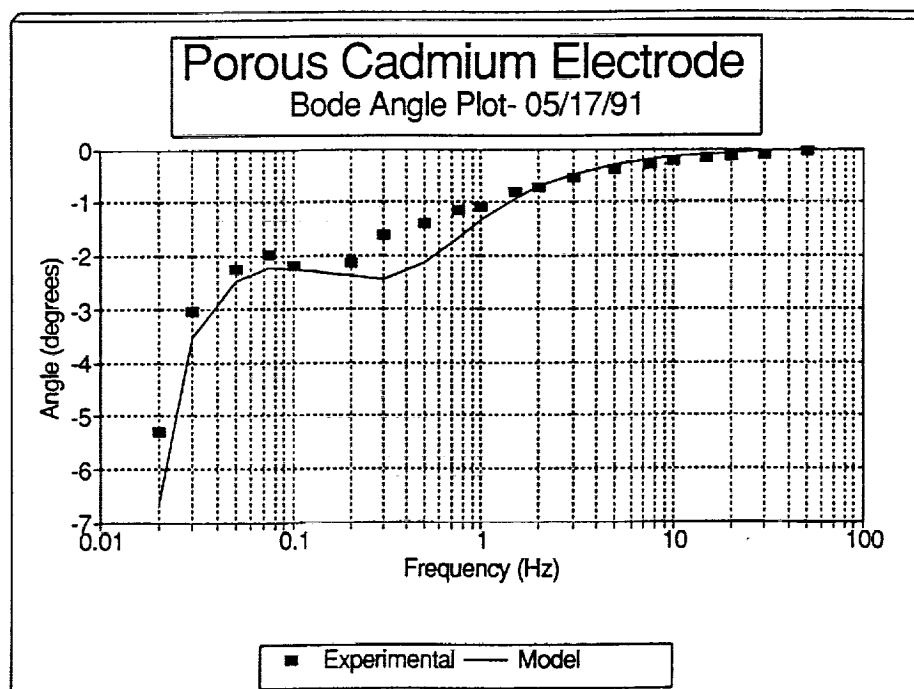

Figure 16. Comparison of experimental and equivalent circuit impedance for a charged cadmium (230 cm^2) electrode (Bode angle plot).
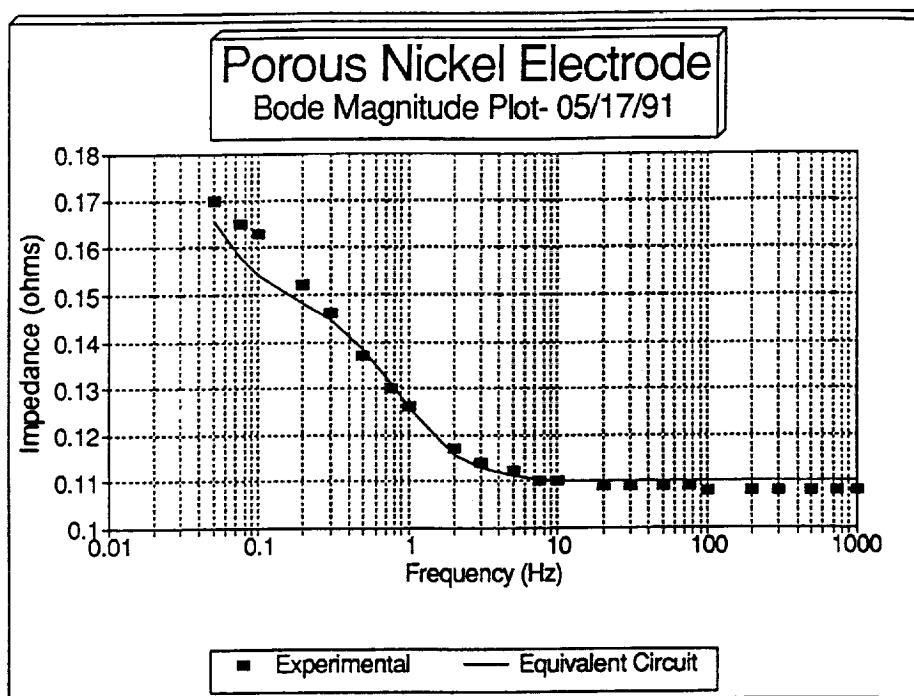
14

Figure 17. Comparison of experimental and equivalent circuit impedance
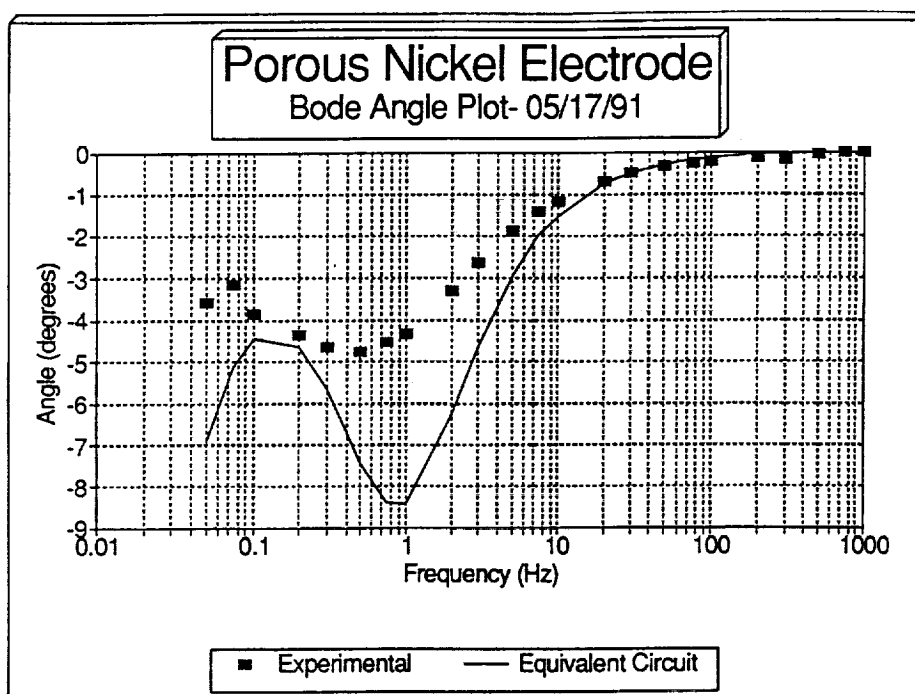for a nickel electrode (230 cm²) (Bode magnitude plot).

Figure 18. Comparison of experimental and equivalent circuit impedance
for a nickel electrode (230 cm²) (Bode angle plot).

Table 1. Equivalent circuit parameters.

	Silver	Nickel	Cadmium
aC	212 F	0.021 F	13.25 F
R_f	0.083 Ω	0.0062 Ω	0.044 Ω
A	2.2×10^{-6} Ω s^{-m}	2.4×10^{-5} Ω s^{-m}	1.7×10^{-5} Ω s^{-m}
m	−1.1	−1.7	−1.9

APPROVAL

TESTING AND ANALYSES OF ELECTROCHEMICAL CELLS USING FREQUENCY RESPONSE

Center Director's Discretionary Fund Final Report, Project No. 90-18

By D.L. Thomas and O.A. Norton Jr.

The information in this report has been reviewed for technical content. Review of any information concerning Department of Defense or nuclear energy activities or programs has been made by the MSFC Security Classification Officer. This report, in its entirety, has been determined to be unclassified.

J.L. RANDALL
Director, Information and Electronic Systems Laboratory

REFERENCES

1. MacDonald, D.D.: "Techniques for Characterization of Electrodes and Electrode Processes." R. Varma and J.R. Selman, ed., John Wiley and Sons, New York, 1991.

2. Newman, J.: "Electrochemical Systems." Second edition, Prentice-Hall, Englewood Cliffs, NJ, 1991.

3. De Levie, R.: "Electrochemica Acta," vol. 8, 1963, p. 751.

4. Missing

5. Missing

6. Armstrong, R.D., and Edmondson, K.: "J. Electroanal. Chem. and Interfacial Electrochem.," vol. 53, 1974, p. 371.

7. Armstrong, R.D., Edmondson, K., and Lee, J.A.: "J. Electroanal. Chem.," vol. 63, 1975, p. 287.

8. Lenhart, S.J., MacDonald, D.D., and Pound, B.G.: "J. Electrochem. Soc.," vol. 135, 1988, p. 1063.

9. Sathyanarayana, S., Venugopalan, S., and Gopikanth, M.L.: "J. Appl. Electrochem.," vol. 9, 1979, p. 125.

10. Zimmerman, A.H., Martinelli, M.R., Janecki, M.C., and Babcock, C.C.: ibid, vol. 129, 1982, p. 289.

11. Tiedemann, W., and Newman, J.: "J. Electrochem. Soc.," vol. 122, 1975, p. 70.